Generic Crystallizer Model: I. A Model Framework for a Well-Mixed Compartment

M. J. Hounslow
Dept. of Chemical and Process Engineering, University of Sheffield, Sheffield S10 2TP, U.K.

A. E. Lewis
Chemical Engineering Department, University of Cape Town, Rondebosch 7701, South Africa

S. J. Sanders
Sanders Simulation, Denville, NJ 07834

R. Bondy
OLI Systems Inc., Morris Plains, NJ 07950

DOI 10.1002/aic.10535
Published online August 3, 2005 in Wiley InterScience (www.interscience.wiley.com).

A model framework is described for crystallization of a single solid species in a well-mixed compartment at steady state. The model framework applies to both Type I (that is, nonhigh yield) crystallization and Type II (high yield) crystallization. The framework consists of population balances incorporating nucleation, growth, aggregation, breakage, classification, and dissolution, coupled with mass and energy balances. The model allows any number of product streams, any number of feed streams, one vapor product stream, nonrepresentative sampling, but only one solid species. The numerical strategy used to solve the resulting set of nonlinear integro-differential equations transforms them into a matrix of algebraic equations. Two algorithms for the solution for Type I crystallization are proposed, both of which consist of solving the material and energy balances sequentially with the population balance and iterating around only one variable. Both algorithms use an existing material and energy balance solution package, which is linked to the population balance equations. The first solution algorithm solves the population balance equations using a Newton–Raphson solver with finite-difference approximations for the derivatives, converging around a variable related to the crystal mass and the number density for each interval. The second algorithm solves the population balance equations using a successive substitution technique with root bracketing and iterates around the suspension density. The choice of algorithm depends on the nature of the system to be modeled. A similar framework is suggested for the solution for Type II crystallization, except that the iteration variable is the growth rate at a fixed supersaturation ratio. © 2005 American Institute of Chemical Engineers *AIChE J,* 51: 2942–2955, 2005

Introduction

This article addresses the specification of a generic model to describe crystallization of a single solid species in a continuous stirred tank as shown in Figure 1. The model uses a structure consisting of input stream data (temperature, pressure, compositions, flow rates, and enthalpies) combined with a function describing the particle size distribution (PSD).

The modeling of a particulate system necessitates the use of the population balance equation (PBE), a statement of continuity for particulate systems, first introduced by Hulbert and Katz[1] and Randolph and Larson.[2,3] The requirements necessary

Correspondence concerning this article should be addressed to M. J. Hounslow at m.j.hounslow@sheffield.ac.uk.

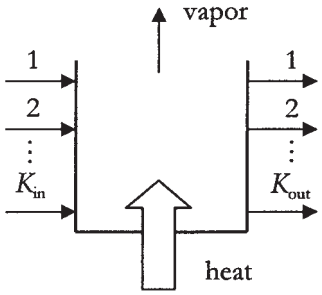

Figure 1. CST.

to completely determine the formation and dynamics of multidimensional particle distributions are covered in Randolph and Larson,[4] Ramkrishna,[5,6] and in extensive detail in Hounslow and Wynn.[7]

There are various techniques available for solving PBEs (see Ramkrishna[5,6] for a general review). In this case, a discretization method is used, which considers the PSD to consist of groups of particles of different sizes, described by a vector of values whose elements correspond to discrete particle sizes. With a given set of input conditions, an appropriate set of operating conditions, and information about crystallization mechanisms, the model can describe the output stream. The real strength of a model such as this is that the solution to the PBE can be coupled to a thermodynamic package such as OLI Systems Inc.[8] or Aspen Plus[9] that rigorously calculates the supersaturation using the comprehensive solution chemistry embodied in such a package.

For this model, there can be K_{in} streams flowing into the vessel, each containing solid, liquid, or solid and liquid. Similarly, there are K_{out} streams flowing out. There is also a stream of vapor leaving and an indirect heat flow.

The model framework allows for nucleation, growth, aggregation, breakage, classification, and dissolution. Destruction of fines can be treated as two coupled crystallizers with classification and dissolution of fines in one of them. It is important to note that this is not an MSMPR (mixed suspension, mixed product removal) model because it is possible to have nonmixed product removal.

Population Balance

Consider the *population balance equation* (PBE) for a continuous stirred tank at steady state. There are K_{in} streams flowing in, at volumetric rates Q_k^{in}, bearing solids with number densities $n_k^{in}(l)$. Similarly, there are K_{out} streams flowing out, at volumetric rates Q_k^{in}, bearing solids with number densities $n_k^{out}(l)$. The tank has a volume V and within the tank the number density is everywhere constant at $n(l)$. This is illustrated in Figure 2.

It must be noted that this representation is incomplete if more than one solid species is present. For processes excluding aggregation, a simple extension is to have a separate number density for each solid; if aggregation is present, a different approach is needed. This latter approach has been developed by Hounslow et al.[10] for two solid systems and can probably be extended to multiple solids if desired. In the work discussed here, it is assumed that only one solid is present.

Within the tank, the state of the solution (such variables as temperature, pressure, and composition) is represented by a vector of state variables, **s**.

The PBE at steady state is

$$\sum_{k=1}^{K_{in}} Q_k^{in} n_k^{in}(l) - \sum_{k=1}^{K_{out}} Q_k^{out} n_k^{out}(l) = Vr[n(\cdot), l, \mathbf{s}] \tag{1}$$

where $r[n(\cdot), l, \mathbf{s}]$ is the density functional describing the net rate of destruction of particles. For most purposes the heart of the PBE is this term, and, provided that $n_k^{out}(l)$ can be written in terms of $n(l)$, the definition of r in terms of $n(l)$ converts Eq. 1 into an equation to be solved for $n(l)$.

Mechanisms

The identification of appropriate kinetic equations for the various mechanisms included in the population balance equation is core to its predictive capacity. Thus, an overview is presented here of some of the models available to describe the various kinetic processes relevant to crystallization. Although the various crystallization mechanisms and kinetics of nucleation and growth, for example, are fundamental to the framework, the choice of function relating the kinetics to the supersaturation and other process variables is of much less importance.

Nucleation. Nucleation is classified as being primary or secondary, depending on the mechanisms through which it occurs.[11] Randolph and Larson[4] consider the phenomenon of nucleation and discuss a number of nucleation models. These range from the fundamental Arrhenius-type expression for the rate of homogeneous nucleation[12] to one accounting for heterogeneous effects.[13] They conclude that an expression based on the Miers nucleation model[14] has been most successful in matching experimental work. The formulation proposed by Randolph and Larson for the nucleation rate B^0, the number of nuclei formed per volume per second, is

$$B^0 = k_{nuc}^{ii}(c - c^*)^I \tag{2}$$

where B^0 is the nucleation rate ($m^{-3}\ s^{-1}$), $k_{nuc}^{ii}$is the nucleation rate constant, c is the solute concentration (kg m^{-3}), and c^* is the equilibrium solute concentration (kg m^{-3}).

It is presumed that k_{nuc}^{ii} can be a function of temperature but that I is not.

Garside[15] proposes an idealization of primary nucleation based on a kinetic law formally identical to the thermodynamic law for homogeneous nucleation (but where the parameters A and B do not have the same physical meaning).

$$B^0 = Ae^{\{-B/[\ln^2(S)]\}} \tag{3}$$

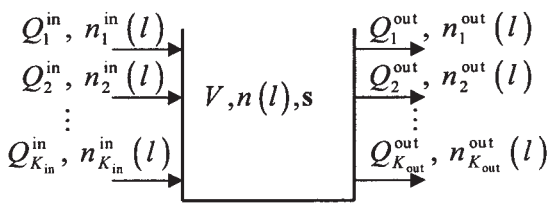

Figure 2. Balance region for PBE.

where S is the supersaturation ratio.

Sohnel and Garside[16] confirm a similar form for primary homogeneous nucleation (applicable over a limited range of supersaturation)

$$B^0 = k_{\text{nuc}}^{iii} S^I = k_{\text{nuc}}^{iv} c^I \tag{4}$$

where B^0 is the nucleation rate (m^{-3} s^{-1}), I is the kinetic "order" of nucleation, S is the supersaturation ratio, c is the solute concentration (kg m^{-3}), and k_{nuc}^{iIi} and k_{nuc}^{iv} are nucleation rate constants (m^{-3} s^{-1} and kg^{-1} s^{-1}, respectively).

Although the nucleation rate constants k_{nuc}^{iIi} and k_{nuc}^{iv} have no physical significance, Eq. 4 is very often used in practice.

Secondary nucleation, besides having an obvious dependency on the level of supersaturation, is generally considered to be related to the suspension density

$$B^0 = k_{\text{nuc}}^{v}(S-1)^I M_T^J \tag{5}$$

where M_T is the suspension density (kg m^{-3}) and k_{nuc}^{v} is the nucleation rate constant (kg^{-1} s^{-1}).

The nucleation rate constant k_{nuc}^{v} is assumed to be related to the stirring power and to exhibit a temperature dependency according to an Arrhenius-type relationship.[17] The exponent I, which does not depend on temperature, lies between 0.5 and 2.5. The exponent J is generally assumed to be of the order of 1 and to depend slightly on temperature.[18]

Gahn and Mersmann[19] proposed a new model for secondary nucleation, in which a direct relationship was formulated between the crystallization kinetics and the frequency and energy of particle–impeller collisions depending on a number of material properties of the crystals. This model has been widely accepted and is expressed as follows

$$B^0 = \lambda_{\text{nuc}}(S-1)^I M_T^J N_{\text{imp}}^k \tag{6}$$

where λ_{nuc} is the secondary nucleation rate constant (m^3 kg^{-2}) and N_{imp} is stirrer speed (s^{-1}).

To assess the predictions of the Gahn–Mersmann[19] model, Bermingham et al.[20] evaluated three additional kinetic models that had also been developed for crystallization processes dominated by secondary nucleation and growth. In these models, inter alia, the attrition rate is not simply a function of the overall crystal concentration, but also of the crystal size distribution. Bermingham concluded that these models,[21-23] although largely empirical, do provide significantly more physical insight into the dominant crystallization phenomena than the traditional power-law models.

Growth. Crystal growth is typically denoted by G, the linear crystal growth rate, and usually has a supersaturation dependency ranging from first to second order depending on the rate-controlling step.[11] McCabe[24] proposed that the linear rate of crystal growth is independent of size, an observation that is conventionally called the ΔL law. If l is defined as a characteristic dimension, then the linear growth rate can be defined as

$$G = \frac{dl}{dt} \tag{7}$$

where G is the linear growth rate (m s^{-1}), l is the characteristic dimension (m), t is time (s), and the mass growth rate is defined as

$$\frac{1}{A}\frac{dm}{dt} = 3\,\frac{k_v}{k_a}\,\rho_s G \tag{8}$$

where A is area of the crystal (m^2), m is mass of the crystal (kg), k_v is the volume shape factor, k_a is the area shape factor, and ρ_s is solid density (kg m^{-3}).

Because crystal growth involves transport of the growth units from the bulk of the solution to the surface of the crystal and the incorporation of those units into the crystal lattice, growth can be controlled by either diffusion or surface integration. Experimental determination of the growth kinetics supported by microscopic examination of crystals often allows determination of the prevailing growth mechanism.[25]

For diffusion-controlled growth (crystallization of compounds with a high solubility, static crystallization, and crystallization from viscous solutions[25]) the growth rate becomes

$$\frac{1}{A}\frac{dm}{dt} = 3\,\frac{k_c}{1-w}\,(c - c^*) \tag{9}$$

where k_c is the mass-transfer coefficient (mol m^{-2} s^{-1}), w is the mass fraction of solute, and $c - c^*$ is the concentration driving force (mol m^{-3}).

The mass-transfer coefficient, $k_c = D_{AB}/\delta$, can be derived from a number of correlations for the Sherwood number, $\text{Sh} = k_c L/D$, such as $\text{Sh} = 2 + 0.6\text{Re}^{1/2}\text{Sc}^{1/3}$,[25] where D_{AB} is the binary diffusion coefficient (mol m^{-1} s^{-1}), δ is the diffusion layer thickness (m), Re is the Reynolds number, and Sc is the Schmidt number.

For surface integration controlled growth, Mullin[26] identified three possible mechanisms: spiral growth, growth by two-dimensional nucleation, and rough growth, of which spiral growth occurs most frequently. The general empirical equation for surface integration controlled growth is[26]

$$G = k_{\text{grow}}(S-1)^I \tag{10}$$

where G is the linear particle growth rate (m s^{-1}) and k_{grow} is the growth rate constant (m s^{-1}).

In the spiral growth mechanism, which occurs at low supersaturation levels, the growth units are incorporated only at kinks on the crystal surface. A defect must first be generated on the surface, whereafter growth proceeds layerwise on this defect. This results in a spiral dislocation, which will continue to propagate as long as growth continues. For spiral growth at very low supersaturations, the exponent in Eq. 10 is $I = 2$ and, for high supersaturations, $I = 1$.[25]

At relatively higher supersaturations, two-dimensional nuclei occur on the crystal surface and the necessary kinks for further growth are generated. This is the two-dimensional nucleation growth mechanism, for which the exponent in Eq. 10 becomes $I > 2$.

At higher supersaturations, growth units can attach themselves anywhere on the crystal surface and the surface becomes rough. In this case, the exponent in Eq. 10 is $I = 1$.

Table 1. Aggregation Kernels after Bramley et al.[35]

Mechanism	Kernel $\beta(l, \lambda)$
Size independent	β_0
Brownian motion (Smoluchowski, 1917)	$\beta_0(l + \lambda)(l^{-1} + \lambda^{-1})$
Gravitational (Berry, 1967)	$\beta_0(l + \lambda)^2(l - \lambda)$
Shear [Smoluchowski (1917) and Low (1975)]	$\beta_0(l + \lambda)^3$
Particle Inertia (Drake, 1972)	$\beta_0(l + \lambda)^2(l^2 - \lambda^2)$
Thompson kernel, empirical (Thompson, 1968)	$\beta_0(l^3 - \lambda^3)/(l^3 + \lambda^3)$

Besides the power-law formulation discussed above, other growth rate formulations are either a size-dependent linear growth rate[27-29] or growth rate dispersion.[30-32]

Aggregation. The first contribution to a model for particle aggregation was from Smoluchowski, who developed an aggregation frequency for particles aggregating by Brownian motion.[33] Subsequently, the practice has been to describe aggregation in terms of an aggregation kernel, a measure of the frequency with which a particle of size l aggregates with one of size λ. Implicit in this description is the assumption that all particle collisions are binary in nature; in other words, the particle concentration is relatively low. Sastry[34] first proposed that the aggregation kernel β be viewed as the product of two factors

$$\beta(L, \lambda) = \beta_0 f(L, \lambda) \tag{11}$$

The first factor, β_0, is the size-independent portion of the rate constant and depends on operating conditions such as the local fluid velocity field and chemical environment, whereas the second factor, $f(L, \lambda)$, is some function of particle size and often reflects the mechanism of aggregation. Table 1[35] summarizes a range of aggregation kernels formulated in this way.

Breakage. Birth and death rates of particles arising from breakage have been defined by Prasher[36] and are reformulated in Nicmanis and Hounslow[37] as number-based quantities. In the rate expressions, the breakage selection rate constant [$S(l, \mathbf{s})$] is the rate at which a fragment of a particle of size l will be selected to break. In the case study by the same workers,[37] a binary breakage function and size-dependent breakage rate are used.

Ramkrishna[5] formulates an ad hoc model for breakage in which breakup of particles occurs independently of each other. The breakage frequency $S(l, r, \mathbf{s}, t)$ is thus sufficient to characterize the rate of destruction of particles of state ($\mathbf{l}$, $\mathbf{r}$) at time t, where $\mathbf{r}$ is the location in physical space and t is time dependency. This formulation is consistent with that suggested by Randolph and Larson[4] in a general description of empirical birth and death processes. For simplicity of formulation, the rate at which particles are selected for breakage can be considered to be independent of spatial position and, at steady state, the time dependency falls away. Hounslow et al.[38] use a breakage function for which there is an analytical solution. The selection rate is taken to increase simply with size cubed and the binary breakage function is formulated as one that gives uniform probability of all fragment sizes on a volume scale. That is

$$S(l, \mathbf{s}) = k_{\text{break}} l^m \tag{12}$$

where S is the breakage selection rate (s^{-1}), k_{break} is the breakage rate constant ($s^{-1}\ m^{-3}$), l is the particle size (m), and

$$b(l, x, \mathbf{s}) = \frac{6x^2}{l^3} \tag{13}$$

Similarly, Attarakih et al.,[39] in their model of droplet breakage, use the following functional form for the breakage selection rate function

$$S(l) = k_{\text{break}} l^m \tag{14}$$

where k_{break} and m are positive parameters. For the daughter droplet distribution, $b(l, x)$ can have two functional forms:

(1) Uniform daughter droplet distribution, where it is assumed that there is an equal chance to form a daughter droplet of any smaller size when a mother droplet breaks up and thus the distribution is independent of daughter droplet volume

$$b(x, l) = \frac{2}{l} \tag{15}$$

(2) Parabolic daughter droplet distribution, where it is assumed that there is a greater or lesser chance to form two daughter droplets of different sizes upon breakage of the mother droplet

$$b(x, l) = \frac{24(x^2 - xl) + 6l^2}{l^3} \tag{16}$$

Classification. A simple approach to classification is to specify the cut size of fines.[4] A more comprehensive approach is to consider segregation as a function of energy dissipation and particle size[11] or to include the effect of superficial flow velocity, flow direction, viscosity, and density difference between the liquid and the solid phases.[11]

Another approach is one where the selection function is a function of size and the state of the vessel contents. The form of the function, applied to stream k, is

$$y_k(l, \mathbf{s}) = H(l - l_0) \tag{17}$$

where $y_k(l, \mathbf{s})$ is the selection function for stream k as a function of size and solution conditions and $H(l - l_0)$ is the Heaviside step function.

In this case, stream k is a representative sample of the bulk for sizes greater than some value l_0, but containing no particles smaller than that size. Thus

$$n_k^{\text{out}} = H(l - l_0) n(l) \tag{18}$$

where n_k^{out} is the number density of stream k out (m^{-4}) and $n(l)$ is the number density of vessel contents (m^{-4}).

The hydrocyclone literature also has some useful size selectivity equations. For example, Plitt and Kawatra[40] propose the following equation for the cut size

$$d_{50(c)} = \frac{14.8 D_c^{0.46} D_i^{0.6} D_o^{1.21} e^{0.063V}}{D_u^{0.71} h^{0.38} Q^{0.45} (\rho_S - \rho_L) 0.5} \tag{19}$$

where $d_{50(c)}$ is the "corrected" d_{50} (μm); D_c, D_i, D_o, and D_u represent the inside diameters of hydrocyclone, inlet, overflow, and underflow, respectively (cm); V is the volumetric percentage of solids in the feed; h is the distance from the bottom of the vortex finder to the top of the underflow orifice (cm); Q is the flow rate of feed slurry ($m^3\ h^{-1}$); and ρ_S and ρ_L represent the density of solids and density of liquid, respectively (g cm^{-1}).

The "corrected" d_{50} is taken from the "corrected" classification curve. The corrected d_{50} is calculated by assuming that, in all classifiers, solids of all sizes are entrained in the coarse product liquid by short-circuiting in direct proportion to the fraction of feed water reporting to the underflow.[41]

Lynch and Rao[42] used weight percent solids, instead of using volume percent solids as in Eq. 19. Their model for calculating cut size is expressed as

$$\log_{10} d_{50(c)} = 0.0173\Phi_w - 0.0695D_u + 0.0130D_o + 0.0048Q + K_1 \quad (20)$$

where Φ_w is the weight percent solids in the feed slurry and K_1 is a constant.

Dissolution. Kramer et al.[43] used the method proposed by Jager[44] where the kinetic dissolution rate is calculated as a function of a mass-transfer coefficient and relative supersaturation. In another work, the same authors[11] observe that dissolution is practically always limited by the mass-transfer step. Both the rate of dissolution and the rate of mass transfer limited growth will thus be limited by the local energy dissipation. Bermingham et al.[20] used a kinetic expression that has a first-order dependency on the supersaturation to describe the dissolution rate in their population balance equation. The rate constant for dissolution is calculated as follows

$$k_c(l) = \frac{D_{AB}}{l}\left[2 + 0.8\left(\frac{\bar{\varepsilon} l^4}{\nu_L^3}\right)^{1/5}\left(\frac{\nu_L}{D_{AB}}\right)^{1/3}\right] \quad (21)$$

where

$$\bar{\varepsilon} = \frac{\mathrm{Ne} N_{\mathrm{imp}}^3 D_{\mathrm{imp}}^5}{V} \quad (22)$$

and k_c is the mass-transfer coefficient (ms^{-1}), D_{AB} is the binary diffusion coefficient ($m^2\ s^{-1}$), l is crystal length (m), ε is the specific power input (W kg^{-1}), ν_L is the kinematic viscosity of the liquid ($m^2\ s^{-1}$), Ne is the power number (also known as the Newton number), N_{imp} is impeller frequency (s^{-1}), D_{imp} is impeller diameter (m), and V is tank volume (m^3).

Dissolution can also be incorporated as a size-independent shrinkage rate constant

$$D(l, s) = D \quad (23)$$

where D is the shrinkage rate constant ($m\ s^{-1}$), or as a mass transfer limited process, as follows

$$D(l, s) = \frac{2k_c(c - c^*)}{\rho_m} \quad (24)$$

where k_c is the mass-transfer coefficient (ms^{-1}), $c - c^*$ is the concentration driving force (mol m^{-3}), and ρ_m is the molar density of particles (mol m^{-3}).

Despite this wealth of information relating to crystallization mechanisms, reporting of modeling studies in the open literature relating to the solution of PBEs tends to fall into one of two categories. In the first category, the studies restrict themselves to a specific system and its measured kinetics and focus on the validation of models with experimental data. In the second category, studies tend to focus on the numerical aspects of solving the PBE, are usually restricted to the very simplest of generic mechanisms, and neglect to use the formulations that are considered to most accurately model the phenomena being considered.

In the first category, numerous studies are presented in the literature. Even the very comprehensive work undertaken by Bermingham et al.[20] is limited to the ammonium sulfate system. In the second category, Kumar and Ramkrishna,[45] in demonstrating a new discretization method for solving PBEs, use their technique to simulate various combinations of initial conditions, nucleation, growth, and aggregation. The functions for all the mechanisms considered are various combinations of exponential and gamma initial distributions; constant, linear, and size-dependent nucleation rates; constant, linear, and size-dependent growth rates; and constant and sum aggregation kernels. Kiparissides and Alexopoulos[46] consider only constant, block pulse, and size-dependent and/or surface area–dependent nucleation rates; constant and size-dependent growth rates; and a Brownian aggregation rate kernel.

This work, however, is proposed to be truly generic, in that practically any chemical system for which there is thermodynamic data may be considered. In addition, the framework incorporates a comprehensive selection of kinetic processes relevant to crystallization and allows the selection of kinetic models for the processes that are believed to most accurately model the various phenomena.

The overall PBE

Once the exit flow term has been modified for classification, and the terms for net rate of destruction attributed to nucleation, growth, dissolution, aggregation, and breakage have been incorporated, the maximal form of the PBE is[47]

$$\sum_{k=1}^{K_{\mathrm{in}}} Q_k^{\mathrm{in}} n_k^{\mathrm{in}}(l) - n(l)\sum_{k=1}^{K_{\mathrm{out}}} Q_k^{\mathrm{out}} y_k(l, \mathbf{s}) = V\Bigg\{-B^0(\mathbf{s}) f^{\mathrm{nuc}}(l, \mathbf{s}) + \frac{d}{dl}[G(l, \mathbf{s})n(l)] + D^0\delta(l) - \frac{d}{dl}[D(l, \mathbf{s})n(l)] - \frac{1}{2}\int_0^l \beta(\sqrt[3]{l^3 - x^3}, x, \mathbf{s})\left(\frac{l}{\sqrt[3]{l^3 - x^3}}\right)^2 n(\sqrt[3]{l^3 - x^3})n(x)dx + n(l)\int_0^\infty \beta(l, x, \mathbf{s})n(x)dx + S(l, \mathbf{s})n(l) - \int_l^\infty S(x, \mathbf{s})b(l, x, \mathbf{s})n(x)dx\Bigg\} \quad (25)$$

subject possibly to the boundary conditions $n(\infty) = n(0^-) = 0$, where

$$y_k(l, \mathbf{s}) \tag{26}$$

is the selection function or grade efficiency and is a function of size and the state of the vessel contents

$$-B^0(\mathbf{s}) f^{\text{nuc}}(l, \mathbf{s}) \tag{27}$$

is the rate of destruction of particles attributed to nucleation

$$+\frac{d}{dl}[G(l, \mathbf{s})n(l)] \tag{28}$$

is the rate of destruction of particles stemming from growth

$$+D^0\delta(l) - \frac{d}{dl}[D(l, \mathbf{s})n(l)] \tag{29}$$

is the rate of destruction of particles attributed to dissolution and $D^0\delta(l)$, the rate of disappearance, is a bookkeeping term to prevent the occurrence of particles of negative size

$$-\frac{1}{2}\int_0^l \beta(\sqrt[3]{l^3 - x^3}, x, \mathbf{s})\left(\frac{l}{\sqrt[3]{l^3 - x^3}}\right)^2 n(\sqrt[3]{l^3 - x^3})n(x)dx \tag{30}$$

is the rate of destruction of particles stemming from aggregation and

$$+S(l, \mathbf{s})n(l) - \int_l^\infty S(x, \mathbf{s})b(l, x, \mathbf{s})n(x)dx \tag{31}$$

is the rate of destruction of particles stemming from breakage.

The moment transformation so often used in the application of PBEs to process models is not possible for arbitrary size dependency. It is, however, possible to make a partial transformation for the third moment

$$m_3 = \int_{0^-}^\infty l^3 n(l)dl \tag{32}$$

Transformation of Eq. 25 gives

$$\sum_{k=1}^{K_{\text{in}}} Q_k^{\text{in}} m_{3k}^{\text{in}} - \sum_{k=1}^{K_{\text{out}}} Q_k^{\text{out}} m_{3k}^{\text{out}}(\mathbf{s}) = V r_3 \tag{33}$$

where

$$r_3[n(\cdot), \mathbf{s}] = \int_{0^-}^\infty l^3 r[n(\cdot), l, \mathbf{s}]dl \tag{34}$$

is a function of $[-B^0(\mathbf{s})f^{\text{nuc}}(\cdot, \mathbf{s}), G(\cdot, \mathbf{s}), D(\cdot, \mathbf{s}), n(\cdot)]$ and $\bar{y}_3(\mathbf{s}) = \int_{0^-}^\infty l^3 y(l, \mathbf{s})dl$.

Replacing the third moment with the suspension density

$$M_T = \rho_S k_V m_3 = \rho_S k_V \int_{0^-}^\infty l^3 n(l)dl \tag{35}$$

gives

$$\sum_{k=1}^{\nu_{\text{in}}} Q_k^{\text{in}} M_{Tk}^{\text{in}} - \sum_{k=1}^{\nu_{\text{out}}} Q_k^{\text{out}} M_{Tk}^{\text{out}} = V\rho_S k_V r_3 \tag{36}$$

This last equation has a crucial role in coupling the material and population balances.

Numerical form of the PBE

Analytical solutions for Eq. 25 are scarcely ever available, so it follows that some numerical strategy will be required. All such numerical strategies known to the authors represent the size distribution at a vector of sizes $\mathbf{l}$, at n_{eq} discrete points

$$\mathbf{l} = (l_1, l_2, \ldots, l_{n_{\text{eq}}}) \tag{37}$$

by n_{eq} discrete values $\mathbf{N}$, related reasonably directly to the number density

$$\mathbf{N} = (N_1, N_2, \ldots, N_{n_{\text{eq}}}) \tag{38}$$

In this report, it is assumed that each of the N_i is the number of particles, per unit volume of suspension, in the size range (l_i, l_{i+1}), that is

$$N_i = \int_{l_i}^{l_{i+1}} n(l)dl \tag{39}$$

In the most sophisticated discretization strategies, the values for $\mathbf{l}$ are chosen and adjusted adaptively by the algorithm as it solves for values for $\mathbf{N}$. This approach offers high accuracy and short execution times at the cost of very complex programming, and is not pursued here. A more tractable family of discretization strategies involves fixing the vector $\mathbf{l}$ for the entire problem. In this case virtually all strategies adopt a geometric discretization of the size axis so that the ratio

$$r = \frac{l_{i+1}}{l_i} = 2^{1/3q} \qquad q \in J^+ \tag{40}$$

is a constant.[47] Satisfactory accuracy for CST problems is usually achieved with $r = 2^{1/3}$ so that, for a 1000-fold range of particle sizes, $n_{\text{eq}} = 30$ is required. (For growth-dominated PFR problems a value of $r = 2^{1/12}$ may be needed in which case, for the same size range $n_{\text{eq}} = 120$ is needed.)

The discretized form of Eq. 33, the *discretized population balance equation* (DPBE), is

$$\sum_{k=1}^{K_{\text{in}}} Q_k^{\text{in}} N_{k,i}^{\text{in}}(l) - \sum_{k=1}^{K_{\text{out}}} Q_k^{\text{out}} N_{k,i}^{\text{out}}(l) = V R_i(\mathbf{N}, \mathbf{s}) \qquad i = 1 \cdots n_{\text{eq}} \tag{41}$$

where $N_{k,i}$ is the number of crystals per unit volume in the kth stream and the ith size interval and R_i is the rate of destruction of particles in the ith size interval. The classification functions relate the exit stream size distributions to the size distribution in the bulk

$$N_{k,i} = y_k(\bar{l}_i)\, N_i \tag{42}$$

where the average size in the ith size interval is

$$\bar{l}_i = \frac{1 + r}{2}\, l_i \tag{43}$$

The discrete forms of Eqs. 35 and 36 are

$$M_T = \rho_S k_V m_3 = \rho_S k_V \sum_{i=1}^{n_{\text{eq}}} \bar{l}_i^3 N_i \tag{44}$$

and

$$\sum_{k=1}^{K_{\text{in}}} Q_k^{\text{in}} M_{Tk}^{\text{in}} - \sum_{k=1}^{K_{\text{out}}} Q_k^{\text{out}} M_{Tk}^{\text{out}} = V \rho_S k_V \sum_{i=1}^{n_{\text{eq}}} \bar{l}_i^3 R_i \tag{45}$$

The task now is to determine expressions for R_i.

Nucleation, growth, and dissolution

To resolve the issue of how to apply the boundary condition at zero size, it is necessary to consider nucleation, growth, and dissolution (ngd) together. Thus, adapting Hounslow et al.[47] to incorporate dissolution

$$R_i^{\text{ngd}} = \begin{cases} D^0 - B^0 f_1^{\text{nuc}} + \dfrac{2}{(1+r) l_1}\left[\left(1 - \dfrac{r^2}{r^2 - 1}\right)(D_1 - G_1) N_1 - \dfrac{r}{r^2 - 1}(D_2 - G_2) N_2\right] & i = 1 \\ -B^0 f_i^{\text{nuc}} + \dfrac{2}{(1+r) l_i}\left[\dfrac{r}{r^2 - 1}(D_{i-1} - G_{i-1}) N_{i-1} + (D_i - G_i) N_i - \dfrac{r}{r^2 - 1}(D_{i+1} - G_{i+1}) N_{i+1}\right] & 1 < i < n_{\text{eq}} \\ -B^0 f_{n_{\text{eq}}}^{\text{nuc}} + \dfrac{2}{(1+r) l_{n_{\text{eq}}}}\left[\dfrac{r}{r^2 - 1}(D_{n_{\text{eq}}-1} - G_{n_{\text{eq}}-1}) N_{n_{\text{eq}}-1} + (D_{n_{\text{eq}}} - G_{n_{\text{eq}}}) N_{n_{\text{eq}}}\right] & i = n_{\text{eq}} \end{cases} \tag{46}$$

The D^0 term, the rate of disappearance, in Eq. 46 is not a constitutive equation, unlike the nucleation rate constant B^0, but just a bookkeeping term to prevent the occurrence of particles of negative size. Further evidence is that the magnitude of D^0 depends on the solution to the PBE, not on conditions in the vessel, such as supersaturation. As shown in Eq. 49, the value of D^0 depends on $n(0^+)$ and cannot be determined without knowledge of that value. By contrast the nucleation rate depends on the state of the vessel.

For the continuous system of equations, the boundary condition to be applied, $n(0^-) = 0$, results in

$$D^0 = \begin{cases} B^0 + [D(0^+, \mathbf{s}) - G(0^+, \mathbf{s})] n(0^+) & f^{\text{nuc}} = \delta(l) \\ [D(0^+, \mathbf{s}) - G(0^+, \mathbf{s})] n(0^+) & f^{\text{nuc}} \text{ continuous} \end{cases} \tag{47}$$

If the rate of growth at zero size is greater than the rate of dissolution, the rate of disappearance will be zero, in which case we have

$$D^0 = \begin{cases} 0 & D(0^+, \mathbf{s}) - G(0^+, \mathbf{s}) < 0 \\ B^0 + [D(0^+, \mathbf{s}) - G(0^+, \mathbf{s})] n(0^+) & f^{\text{nuc}} = \delta(l) \\ [D(0^+, \mathbf{s}) - G(0^+, \mathbf{s})] n(0^+) & f^{\text{nuc}} \text{ continuous} \end{cases} \tag{48}$$

It is probably most sensible to apply this equation on the first size interval and to represent n by a first-order difference, in which case

$$D^0 = \begin{cases} 0 & D_1 - G_1 < 0 \\ B^0 + (D_1 - G_1)\dfrac{N_1}{l_2 - l_1} & f^{\text{nuc}} = \delta(l) \\ (D_1 - G_1)\dfrac{N_1}{l_2 - l_1} & f^{\text{nuc}} \text{ continuous} \end{cases} \tag{49}$$

Aggregation

The full form for arbitrary q, given by Litster et al.[48] and refined by Wynn, is[49]

$$R_i^{\text{agg}} = -\sum_{j=1}^{i-\Delta_1} \beta_{i-1,j} N_{i-1} N_j \frac{2^{(j-i+1)/q}}{2^{1/q} - 1} - \sum_{p=2}^{q} \sum_{j=i-\Delta_{p-1}}^{i-\Delta_p} \beta_{i-p,j} N_{i-p} N_j \frac{2^{(j-i+1)/q} - 1 + 2^{-(p-1)/q}}{2^{1/q} - 1}$$

$$-\frac{1}{2}\beta_{i-q,i-q}N_{i-q}^2$$

$$-\sum_{p=1}^{q-1}\sum_{j=i+1-\Delta_{p+1}}^{i+1-\Delta_p}\beta_{i-p,j}N_{i-p}N_j\frac{-2^{(j-i)/q}+2^{1/q}-2^{-p/q}}{2^{1/q}-1}$$

$$+\sum_{j=1}^{i-\Delta_1+1}\beta_{i,j}N_iN_j\frac{2^{(j-i)/q}}{2^{1/q}-1}+\sum_{j=i-\Delta_1+2}^{\infty}\beta_{i,j}N_iN_j \quad (50)$$

where

$$\Delta_p=\mathrm{Int}\left[1-\frac{q\ln(1-2^{-p/q})}{\ln 2}\right] \quad (51)$$

and Int[x] subtracts the fractional part (if any) from x. Note that care must be taken here when calculating the value of Δ_p because of rounding errors when the integer part of the calculated expression is extracted.

Breakage

The discrete form developed by Hounslow et al.[38] is

$$R_i^{\mathrm{break}}=S_iN_i-\sum_{j=i}^{n_{\mathrm{eq}}}b_{i,j}S_jN_j \quad (52)$$

Although this seems a very simple recasting of the continuous form of the equation, it must be understood that the S_i and $b_{i,j}$ cannot be deduced by evaluating the continuous functions at $\bar{l}_i$ and $\bar{l}_j$. Instead, a more complicated process is required (see Eqs. 31 and 34 in Hounslow et al.[38]).

Solving the DPBE

The maximal form of the DPBE is obtained by combining Eq. 41 with Eqs. 42, 46, 50, and 52

$$\sum_{k=1}^{K_{\mathrm{in}}}Q_k^{\mathrm{in}}N_{k,i}^{\mathrm{in}}-N_i\sum_{k=1}^{K_{\mathrm{out}}}Q_k^{\mathrm{out}}y_{k,i}=VR_i(\mathbf{N},\mathbf{s})=V(R_i^{\mathrm{ngd}}+R_i^{\mathrm{agg}}+R_i^{\mathrm{break}}) \qquad i=1\cdots n_{\mathrm{eq}} \quad (53)$$

For a problem where the feed size distributions are given, Eq. 53 provides n_{eq} equations in n_{eq} unknowns: that is, the vector of N_i values, $\mathbf{N}$. Solving the DPBE is then a matter of solving these n_{eq} equations for these n_{eq} unknowns.

Irrespective of the sophistication of the method or fineness of the discretization used, Eq. 25 is transformed into n_{eq} simultaneous nonlinear algebraic equations

$$a_i+\mathbf{B}_i\mathbf{N}+\mathbf{N}^T\mathbf{C}_i\mathbf{N}=0 \qquad i=1,2,\ldots,n_{\mathrm{eq}} \quad (54)$$

where a_i is a (different) constant for each equation, $\mathbf{B}_i$ is a (different) vector of constants (of length n_{eq}) for each equation, and $\mathbf{C}_i$ is a (different) matrix of size $n_{\mathrm{eq}}\times n_{\mathrm{eq}}$ for each equation.

Embedded within this is the discrete equivalent of Eq. 42

$$N_{i,k}=y_{k,i}N_i \quad (55)$$

The suspension density is calculated from

$$M_T=\rho_S k_{\mathrm{V}}\sum_{i=1}^{n_{\mathrm{eq}}}\bar{l}_i^3N_i \quad (56)$$

There are two possible solution strategies for the discretized population balance equations. The most obvious solution strategy is to solve the $(n_{\mathrm{eq}}+1)$ equations using a simple nonlinear equation solver with numerical estimation of the Jacobian (where the extra equation is Eq. 56). This has been found to be a robust and simple-to-implement technique[50] and this is one of the strategies that has been adopted here. A Newton–Raphson technique has been implemented, with finite-difference approximations for the derivatives. The system of equations is "dense" because all equations involve all unknowns. Nonetheless, robust convergence is obtained even with poor initial estimates of the solution and a numerical Jacobian. However, the expense of evaluating the Jacobian is considerable, and so other approaches are desirable.

The second solution strategy uses the observation that, in the absence of aggregation, Eq. 53 is in fact linear in $\mathbf{N}$. With that observation, it is useful to write Eq. 53, with the results of Eqs. 46 and 52 but without Eq. 50 shown explicitly. For example, with $1<i<n_{\mathrm{eq}}$, this becomes

$$\sum_{k=1}^{K_{\mathrm{in}}}Q_k^{\mathrm{in}}N_{k,i}^{\mathrm{in}}-N_i\sum_{k=1}^{K_{\mathrm{out}}}Q_k^{\mathrm{out}}y_{k,i}=V\Bigg\{-B^0f_i^{\mathrm{nuc}}+\frac{2}{(1+r)l_i}\Bigg[\frac{r}{r^2-1}(D_{i-1}-G_{i-1})N_{i-1}+(D_i-G_i)N_i-\frac{r}{r^2-1}(D_{i+1}-G_{i+1})N_{i+1}\Bigg]+S_iN_i-\sum_{j=1}^{n_{\mathrm{eq}}}b_{i,j}S_jN_j+R_i^{\mathrm{agg}}\Bigg\}$$

This equation, and the results for $i=1$ and $i=n_{\mathrm{eq}}$, may be written as a set of equations

$$\mathbf{A}+\mathbf{B}\mathbf{N}=0 \quad (57)$$

where $\mathbf{A}$ is a column vector of length n_{eq} and $\mathbf{B}$ is an $n_{\mathrm{eq}}\times n_{\mathrm{eq}}$ matrix that can be decomposed into two matrices, $\mathbf{E}$ a tridiagonal matrix and $\mathbf{F}$ an upper-right triangular matrix

$$\mathbf{B}=\mathbf{E}+\mathbf{F} \quad (58)$$

$$\mathbf{A}=\begin{bmatrix}A_1\\A_2\\\vdots\\A_{n_{\mathrm{eq}}}\end{bmatrix} \quad (59)$$

$$\mathbf{E} = \begin{bmatrix} b_1 & c_1 & 0 & \cdots & \cdots & 0 \\ a_2 & b_2 & c_2 & & & \vdots \\ 0 & a_3 & b_3 & c_3 & & \vdots \\ \vdots & & \ddots & \ddots & \ddots & \vdots \\ \vdots & & & a_{n_{\mathrm{eq}}-1} & b_{n_{\mathrm{eq}-1}} & c_{n_{\mathrm{eq}}-1} \\ 0 & \cdots & \cdots & \cdots & a_{n_{\mathrm{eq}}} & b_{n_{\mathrm{eq}}} \end{bmatrix} \tag{60}$$

$$\mathbf{F} = \begin{bmatrix} F_{1,1} & F_{1,2} & F_{1,3} & \cdots & \cdots & F_{1,n_{\mathrm{eq}}} \\ 0 & F_{2,2} & F_{2,3} & \cdots & \cdots & F_{2,n_{\mathrm{eq}}} \\ 0 & 0 & F_{3,3} & & & \vdots \\ \vdots & & \ddots & \ddots & \ddots & \vdots \\ \vdots & & & 0 & F_{n_{\mathrm{eq}}-1,n_{\mathrm{eq}}-1} & F_{n_{\mathrm{eq}}-1,n_{\mathrm{eq}}} \\ 0 & \cdots & \cdots & \cdots & 0 & F_{n_{\mathrm{eq}},n_{\mathrm{eq}}} \end{bmatrix} \tag{61}$$

and the elements of **A** and **B** are

$$A_i = \begin{cases} -\sum_{k=1}^{K_{\mathrm{in}}} Q_k^{\mathrm{in}} N_{k,1}^{\mathrm{in}} - VB^0 f_1^{\mathrm{nuc}} + VD^0 + VR_1^{\mathrm{agg}} & i = 1 \\ -\sum_{k=1}^{K_{\mathrm{in}}} Q_k^{\mathrm{in}} N_{k,i}^{\mathrm{in}} - VB^0 f_i^{\mathrm{nuc}} + VR_i^{\mathrm{agg}} & 1 < i \le n_{\mathrm{eq}} \end{cases} \tag{62}$$

$$a_i = \frac{2Vr(D_{i-1} - G_{i-1})}{(1+r)(r^2-1)l_i} \qquad 1 < i \le n_{\mathrm{eq}} \tag{63}$$

$$b_i = \begin{cases} \dfrac{2V(D_1 - G_1)}{(1+r)(r^2-1)l_1} + VS_1 + \sum_{k=1}^{K_{\mathrm{out}}} Q_k^{\mathrm{out}} y_{k,1} & i = 1 \\ \dfrac{2V(D_i - G_i)}{(1+r)l_i} + VS_i + \sum_{k=1}^{K_{\mathrm{out}}} Q_k^{\mathrm{out}} y_{k,i} & 1 < i \le n_{\mathrm{eq}} \end{cases} \tag{64}$$

$$c_i = -V \frac{2}{(1+r)l_i} \frac{r}{r^2-1} (D_{i+1} - G_{i+1}) \qquad 1 \le i < n_{\mathrm{eq}} \tag{65}$$

$$F_{i,j} = -Vb_{i,j}S_j \qquad 1 \le i \le n_{\mathrm{eq}}; j \ge i \tag{66}$$

It may be seen that, for any one set of conditions for which the DPBE is to be solved, **B** is a constant, from which it follows that $\mathbf{B}^{-1}$ is also a constant. On the other hand, **A** depends on the aggregation rate, which in turn depends on **N** by Eq. 50. The strategy is to invert Eq. 57 to give

$$\mathbf{N} = -\mathbf{B}^{-1}\mathbf{A}(\mathbf{N}) \tag{67}$$

where now **A** is shown explicitly to be a function of **N**. Equation 67 may be applied iteratively using the following algorithm:

1. Assemble **B**
2. Find $\mathbf{B}^{-1}$
3. While **N** is changing, Do:
   a. Calculate **A**
   b. Determine **N** from Eq. 67
4. Exit

Table 2. Stream Definitions

Variable	Unit	Symbol	Stream Type SL	Stream Type V
Temperature	°C	T	●	●
Pressure	Pa	P	●	●
Total flow	mol s^{-1}	$\dot{n}_{\mathrm{T}}$	●	●
Total solid flow	mol s^{-1}	$\dot{n}_{\mathrm{ST}}$	●	
Total liquid flow	mol s^{-1}	$\dot{n}_{\mathrm{LT}}$	●	
Liquid species flows	mol s^{-1}	$\dot{\mathbf{n}}_{\mathrm{L}} = (\dot{n}_{\mathrm{L}_1}, \dot{n}_{\mathrm{L}_2}, \ldots, \dot{n}_{\mathrm{L}_J})$	●	
Solid species flows	mol s^{-1}	$\dot{\mathbf{n}}_{\mathrm{S}} = (\dot{n}_{\mathrm{S}_1}, \dot{n}_{\mathrm{S}_2}, \ldots, \dot{n}_{\mathrm{S}_J})$	●	
Vapor species flows	mol s^{-1}	$\dot{\mathbf{n}}_{\mathrm{V}} = (\dot{n}_{\mathrm{V}_1}, \dot{n}_{\mathrm{V}_2}, \ldots, \dot{n}_{\mathrm{V}_J})$		●
Volumetric flow	m^3 s^{-1}	Q	●	
Specific enthalpy	J mol^{-1}	H	●	●
Size distribution	m^{-3}	$\mathbf{N} = (N_1, N_2, \ldots, N_{n_{\mathrm{eq}}})$	●	

The Material and Energy Balances

Stream data

Representation of two types of streams is included: solid–liquid streams and vapor-only streams. Within each stream data specification, flows are represented as species molar flows for each phase and some redundant data are included to prevent frequent recalculation. For a system containing J species the stream specifications are as shown in Table 2.

The material balance

The material balance states simply that the molar flow in of each species equals the molar flow out of that species

$$\sum_{k=1}^{K_{\mathrm{in}}} \dot{\mathbf{n}}_{\mathrm{T}_k}^{\mathrm{in}} - \sum_{k=1}^{K_{\mathrm{out}}} \dot{\mathbf{n}}_{\mathrm{T}_k}^{\mathrm{out}} - \dot{\mathbf{n}}_{\mathrm{V}} = \boldsymbol{\nu}\dot{\boldsymbol{\zeta}} \tag{68}$$

where $\boldsymbol{\nu}$ is a matrix of stoichiometric coefficients for the E independent solution-phase chemical reactions taking place with reaction rates given by the vector $\dot{\boldsymbol{\xi}}$. Note that the production of solid does not count as a reaction here, given that Eq. 68 counts, for example, NaCl(aq) with the same species number as that of NaCl(s). The rate of generation of solid can be deduced from the PBE, Eq. 25. The mass balance couples directly to the PBE by the suspension density M_T, as given in Eq. 36, which in turn can be related to the molar flows as follows

$$M_{T,k} = \frac{\sum_i M_{\mathrm{R},i} \dot{\mathbf{n}}_{\mathrm{S}_{k,i}}}{\frac{1}{\rho_{\mathrm{S}}} \sum_i M_{\mathrm{R},i} \dot{n}_{\mathrm{S}_{k,i}} + \frac{1}{\rho_{\mathrm{L}}} \sum_i M_{\mathrm{R},i} \dot{n}_{\mathrm{L}_{k,i}}} \tag{69}$$

where $M_{\mathrm{R},i}$ is the relative molar mass for species i and ρ_{S} and ρ_{L} are the mass densities for the solid and liquid phases, respectively.

It will usually be the case that the solution composition of all exiting liquid streams will be the same so that, if the mol fractions of each species in solution in the vessel are $\mathbf{x}$, then

$$\frac{\dot{n}_{\mathrm{L}_{k,i}}}{\dot{n}_{\mathrm{LT}_k}} = x_i \tag{70}$$

where $\dot{n}_{\mathrm{LT}_k}$ is the total molar flow of liquid in stream k. The total flow for each stream is

$$\dot{n}_{\mathrm{T}_k} = \dot{n}_{\mathrm{ST}_k} + \dot{n}_{\mathrm{LT}_k} \tag{71}$$

Similarly, if the solid has mol fractions $\mathbf{x}_\mathrm{S}$

$$\frac{\dot{n}_{\mathrm{S}_{k,i}}}{\dot{n}_{\mathrm{ST}_k}} = \mathrm{x}_{\mathrm{S}_i} \tag{72}$$

and the vapor mol fractions $\mathbf{x}^{\mathrm{vap}}$

$$\frac{\dot{n}_i^{\mathrm{vap}}}{\dot{n}_\mathrm{T}^{\mathrm{vap}}} = x_i^{\mathrm{vap}} \tag{73}$$

The volume flow rate for the solid–liquid streams may be determined from

$$Q_k = \sum_{i=1}^{J} M_{\mathrm{R},i}\left(\frac{\dot{n}_{\mathrm{S}_{k,i}}}{\rho_\mathrm{S}} + \frac{\dot{n}_{\mathrm{L}_{k,i}}}{\rho_\mathrm{L}}\right) \tag{74}$$

The energy balance

The energy balance can be written most succinctly in terms of the specific enthalpies H. The balance is

$$\sum_{k=1}^{K_{\mathrm{in}}} \dot{n}_{\mathrm{T}k}^{\mathrm{in}} H_k^{\mathrm{in}} - \sum_{k=1}^{K_{\mathrm{out}}} \dot{n}_{\mathrm{T}k}^{\mathrm{out}} H_k^{\mathrm{out}} - \dot{n}_\mathrm{T}^{\mathrm{vap}} H^{\mathrm{vap}} = -q \tag{75}$$

It is to be expected that the specific enthalpy of the solution and of the solids in each of the exit streams will be the same as that in the vessel, that is,

$$\dot{n}_{\mathrm{T}_k} H_k = \dot{n}_{\mathrm{TS}_k} H_\mathrm{S} + \dot{n}_{\mathrm{TL}_k} H_\mathrm{L} \tag{76}$$

In addition, it is assumed that all exit streams have the same temperature and pressure as those of the vessel

$$T_k^{\mathrm{out}} = T^{\mathrm{vap}} = T \qquad P_k^{\mathrm{out}} = P^{\mathrm{vap}} = P \tag{77}$$

Solving the Balance Equations

Problem specification

A standard specification would be

- Complete description of the feedstreams
- Total flow rates of all but one of the solid–liquid exit streams
- Crystallization kinetic equations: $B^0(\mathbf{s})$, $f^{\mathrm{nuc}}(l, \mathbf{s})$, $G(l, \mathbf{s})$, $D(l, \mathbf{s})$, $\beta(l, x, \mathbf{s})$, $S(l, \mathbf{s})$, $b(l, x, \mathbf{s})$
- Heat input, q
- Vessel size, V
- Selection functions $y_k(l)$
- Composition of the vapor stream
- Vessel operating pressure

Unknowns to be determined

The model must then determine the complete specification of the product streams

- Solid liquid streams: $(7 + 2J + n_{\mathrm{eq}}) \times K_{\mathrm{out}}$ variables
- Vapor stream: $4 + J$
- Vessel conditions: T, $\mathbf{x}$, H_S, H_L, M_T, $\dot{\mathrm{X}}\boldsymbol{\xi}$, $\mathbf{N}$, that is, $3 + J + E + n_{\mathrm{eq}}$ (note that $\mathbf{x}$ counts as $J - 1$ unknowns)
- The rate constants, such as B^0, G^0, D, β, S (that is, 5)

The total number of unknowns is: $(7 + 2J + n_{\mathrm{eq}}) \times (K_{\mathrm{out}} + 1) + 5 + E$

Equations available

In Table 3, the available equations for a Type I (that is, nonhigh yield) crystallization are presented. So, for example, for a system

- with three cations, three anions, four complexes, and water, that is, $J = 11$
- four independent reactions, $E = 4$
- two exit streams, that is, $K_{\mathrm{out}} = 2$
- $n_{\mathrm{eq}} = 30$

the total number of equations to be solved is $(7 + 22 + 30) \times (2 + 1) + 5 + 4 = 186$. For a Type II, or high-yield system, one of the kinetics equations would be lost, and an additional equilibrium equation (for the solid) asserted.

Tearing

There are many commercial thermodynamic modules that allow the solution of material and energy balance problems,[8,9] so it seems sensible to use these and therefore to deconstruct the problem between the thermodynamic calculations on the one hand and the population balances on the other hand. The supersaturation ratio is calculated at a fixed T, P, composition, and mass of crystal precipitated. The supersaturation ratio then allows the calculation of the kinetic parameters to be used in the solution of the population balances. In fact, this is the real strength of a model such as this. Coupling the solution to the PBE to a thermodynamic package means that the supersaturation is rigorously calculated on the basis of the comprehensive solution chemistry embodied in such a package.

The solution of the population balances then allows the calculation of a new vector of number of particles ($\mathbf{N_i}$) and the mass of crystal precipitated from the suspension density.

Thus, for Type I systems, the iteration occurs over $(n_{eq} + 1)$ variables. For Type II systems, the algorithm still applies, but it is necessary to iterate over the growth rate.

Type I Systems: Newton–Raphson Solution Algorithm

1. Estimate M_c, the total crystal mass in the crystallizer produced by crystallization, by varying M_c to match the user-specified estimate of the supersaturation ratio. Compute u_{mc}, a transform of M_c, as follows

$$u_{mc} = -\ln\left(1 - \frac{M_c}{M_{cmax}}\right) \tag{78}$$

Table 3. Equations Available

Source	Equation	Instances
Thermodynamics	$H_L(T, P, \mathbf{x})$	1
	$H_S(T, P)$	1
	$H^{vap}(T, P, \mathbf{x}^{vap})$	1
	$T(P, \mathbf{x})$	1
	Equilibria	E
Population balance	**54**	n_{eq}
Kinetics	Given	5
Classification	**55**	$n_{eq} \times K_{out}$
Material balance	68	J
Solid flow	**56**, 69	K_{out}
Definition of suspension density	**56**	1
Solution composition	70	$J \times K_{out}$
Total flows	71	K_{out}
Solid composition	72	$J \times K_{out}$
Energy balance	75	1
Steam enthalpies	76	K_{out}
Equilibration of T and P	77	$2(K_{out} + 1)$
Vapor species flows	73	J
Exit flows	Given	$K_{out} - 1$
Volume flows	74	K_{out}
Total		$(7 + 2J + n_{eq}) \times (K_{out} + 1) + 5 + E$

This transform prevents M_c from exceeding the maximum amount of solute available M_{cmax} and is used only for this purpose in the algorithm. For classified product removal, the calculated value of M_{cmax} is the same as that for mixed product removal because it is merely used as the upper numerical bound.

2. Estimate a starting value for $\mathbf{N_i}$ such that M_T (suspension density) $= M_c/V_m$.

3. Calculate M_T, the suspension density, for the current set of N_i values.

4. Calculate the supersaturation ratio S for the current value of M_c, the mass of crystal precipitated.

5. Calculate the predicted value of the mass of crystal precipitated, M_{c_calc} from

$$M_{c\_calc} = \frac{M_T V_m}{1 - \left(\frac{M_T}{\rho_c}\right)} \tag{79}$$

6. Calculate the kinetic rate constants from the vector **s**.

7. Compute the error for RHS(i) as $\sqrt{\sum}$ {[RHS(i) of Eq. 48]^2}. Compute the error for RHS($n_{eq} + 1$) $= M_c - M_{c\_calc}$.

8. Compute the derivatives d(Eq. 53)/$d\mathbf{N_i}$ using finite differences.

9. Compute the derivatives d(Eq. 53)/du_{mc}.

10. Compute corrections to the $\mathbf{N_i}$ and u_{mc} from the solution of

$$\mathbf{Ax} = \mathbf{b}$$

where **A** is the the Jacobian; **b** is the RHS vector of errors in the material and energy balances and $M_c - M_{c\_calc}$; **x** represents corrections to the variables $\mathbf{N_i}$ and u_{mc}, designated $\mathbf{\Delta N_i}$ and Δu_{mc}.

11. Set $\alpha = 1$.

12. Update $\mathbf{N_i}$ using $\mathbf{N_i(k + 1)} = \mathbf{N_i(k)} + \boldsymbol{\alpha}(\mathbf{\Delta N_i})$ and $u_{mc}(k + 1) = u_{mc}(k) + \alpha(\Delta u_{mc})$, where k is the iteration number.

13. Compute M_c from

$$M_c = M_{cmax}[1 - \exp(-u_{mc})] \tag{80}$$

14. Compute a new error using steps 3–8.

15. If the error was reduced, check for convergence. In this case, the tolerance is 1.0E-6. If converged, exit.

16. If the error was reduced but not converged, go to step 3 and calculate another Newton step.

17. If the error was not reduced, set $\alpha = \alpha/4$ and go to step 12 to take a shorter step in the direction of the Newton correction.

Type I Systems: Successive Substitution with Root-Bracketing Solution Algorithm. The root–bracketing algorithm below is used to solve Eq. 36 for the suspension density M_T.

1. Perform a mass and energy balance assuming no solid is precipitated.
   a. Denote M_T as M_T^0.
   b. Calculate the kinetic rate constants from the vector **s**.
   c. Solve the PBE; note the error in Eq. 36 as Δ^0.
2. Perform a mass and energy balance assuming solid is precipitated to form a saturated solution.
   a. Denote M_T as M_T^{max}.
   b. Calculate the kinetic rate constants from the vector **s**.
   c. Solve the PBE; note the error in Eq. 36 as Δ^{max}
3. If $\Delta^0 \times \Delta^{max} > 0$, exit with error.
4. If $\Delta^0 < 0$,
   a. then set $M_T^1 = M_T^0$, $M_T^2 = M_T^{max}$, $\Delta^1 = \Delta^0$, $\Delta^2 = \Delta^{max}$
   b. else set $M_T^1 = M_T^{max}$, $M_T^2 = M_T^0$, $\Delta^1 = \Delta^{max}$, $\Delta^2 = \Delta^0$
5. Set $M_T = 0.5(M_T^1 + M_T^2)$.
   a. Solve the material and energy balance with the mass precipitated corresponding to M_T.
   b. Calculate the kinetic rate constants from the vector **s**.
   c. Solve the PBE; note the error in Eq. 36 as Δ.
   d. If $\Delta \times \Delta^1 > 0$,
      i. then $M_T^1 = M_T$, $\Delta^1 = \Delta$
      ii. else $M_T^2 = M_T$, $\Delta^2 = \Delta$
6. Do While $|\Delta| > \text{tol.} \times |\Delta^0|$

a. $M_T = 0.5(M_T^1 + M_T^2)$.
b. Solve the material and energy balance with the mass precipitated corresponding to M_T.
c. Calculate the kinetic rate constants from the vector **s**.
d. Solve the PBE; note the error in Eq. 36 as Δ.
e. If $\Delta \times \Delta^1 > 0$,
i. then $M_T^1 = M_T$, $\Delta^1 = \Delta$
ii. else $M_T^2 = M_T$, $\Delta^2 = \Delta$
7. Exit.

For type I crystallization, the choice of the most appropriate algorithm depends on the nature of the system to be modeled. For cases where the index of aggregation (I_{agg}) is small, where $I_{agg} = 1 - (m_0/B_0\tau) < 0.333$, it is appropriate to use the successive substitution method because this will converge economically and rapidly. For cases with higher indices of aggregation, the Newton–Raphson solver is more appropriate, given that the nonlinearity introduced by the aggregation terms becomes more significant. This is covered in more detail in a subsequent article.

Type II Systems: Successive Substitution with Root-Bracketing Solution Algorithm. The root-bracketing algorithm below is used to solve Eq. 36 for the size-independent portion of the growth rate G_0, starting from a pair of first guesses $(0, G_0^{max})$
1. Perform a mass and energy balance with solid precipitated to form a saturated solution.
2. Solve the PBE with $G_0 = G_0^0 = 0$; note the error in Eq. 36 as Δ^0.
3. Solve the PBE with $G_0 = G_0^{max}$; note the error in Eq. 36 as Δ^{max}.
4. Do While $\Delta^0 \times \Delta^{max} > 0$
a. $G_0^{max} = 2G_0^{max}$.
b. Solve the PBE with $G_0 = G_0^{max}$; note the error in Eq. 36 as Δ^{max}.
5. If $\Delta^0 < 0$,
a. then set $G_0^1 = G_0^0$, $G_0^2 = G_0^{max}$, $\Delta^1 = \Delta^0$, $\Delta^2 = \Delta^{max}$
b. else set $G_0^1 = G_0^{max}$, $G_0^2 = G_0^0$, $\Delta^1 = \Delta^{max}$, $\Delta^2 = \Delta^0$.
6. Set $G_0 = 0.5(G_0^1 + G_0^2)$.
a. Solve the PBE; note the error in Eq. 36 as Δ.
b. If $\Delta \times \Delta^1 > 0$,
i. then $G_0^1 = G_0$, $\Delta^1 = \Delta$
ii. else $G_0^2 = G_0$, $\Delta^2 = \Delta$.
7. Do While $|\Delta| > \text{tol.} \times |\Delta^0|$
a. $G_0 = 0.5(G_0^1 + G_0^2)$.
b. Solve the PBE; note the error in Eq. 36 as Δ.
c. If $\Delta \times \Delta^1 > 0$,
i. then $G_0^1 = G_0$, $\Delta^1 = \Delta$
ii. else $G_0^2 = G_0$, $\Delta^2 = \Delta$.
8. Exit.

Conclusions

The modeling of a single continuous stirred tank crystallizer with any number (>1) of product streams, any number of feed streams, one vapor product stream, nonrepresentative sampling, and only one solid species has been described.

The mechanisms allowed are nucleation, growth, aggregation, dissolution, breakage, and classification.

The model constitutes coupled material, energy, and population balance equations.

The population balance equation, Eq. 25, serves two roles:

(1) It links the size distribution from a crystallizer to the kinetics of the processes taking place in that crystallizer.

(2) It couples the kinetics to the mass balance equation, by enabling calculation of the mass of solid produced.

Solution of the PBE requires both conversion to a discrete form as well as numerical solution of the discrete form. Two algorithms for the solution of the resulting matrix of algebraic equations are proposed: The first solves the population balance equations using a Newton–Raphson solver with finite-difference approximations for the derivatives, converging around a variable related to the crystal mass and N_i for each size interval. The second uses a successive substitution technique with root bracketing and iterates around the suspension density. The choice of the most appropriate algorithm depends on the nature of the system to be modeled. A similar framework is suggested for the solution for Type II crystallization, except that the iteration variable is the growth rate at a fixed supersaturation ratio.

Acknowledgments

This work was supported by the EPSRC of the United Kingdom, OLI Systems Inc., and the National Research Foundation of South Africa.

Notation

a = a coefficient, Eq. 54
a = component of **E**
A = component of **A**
A = parameter in Eq. 3
A = area of crystal, m^2
b = component of **B** and **E**
$b(l, x, \mathbf{s})$ = breakage function, m^{-1}
B = parameter in Eq. 3
$B^0(\mathbf{s})$ = nucleation rate, $m^{-3}\ s^{-1}$
c = component of **C**
c = component of **E**
c = solute concentration, kg m^{-3}
c^* = equilibrium solute concentration, kg m^{-3}
$d_{50(c)}$ = "corrected" d_{50} for the hydrocyclone (Eq. 19), μm
D = shrinkage rate constant in Eq. 23, m s^{-1}
$D(l, \mathbf{s})$ = linear rate of shrinkage, m s^{-1}
D^0 = rate of disappearance, m−3 s^{-1}
D_{AB} = binary diffusion coefficient ($m^2\ s^{-1}$) in calculating k_c in Eq. 9, mol $m^{-1}\ s^{-1}$
D_{imp} = impeller diameter, m
$D_{c,\ Di,\ Do,\ Du}$ = inside diameters of hydrocyclone, inlet, vortex finder, and apex, respectively (Eq. 19), cm
E = number of independent reactions
$f^{nuc(l,\ \mathbf{s})}$ = the nuclei size distribution, m^{-1}
f_i^{nuc} = the discrete equivalent of $f^{nuc}(l, \mathbf{s})$
F = component of **F**
$G(l, \mathbf{s})$ = linear rate of crystal growth, m s^{-1}
G_0^{max} = maximum guessed value for growth rate, m s^{-1}
H = specific enthalpy, J mol^{-1}
H = Heaviside step function in Eq. 17
h = the distance from the bottom of the vortex finder to the top of the underflow orifice in the hydrocyclone (Eq. 19), cm
i = a size class
I_{agg} = index of aggregation, $I_{agg} = 1 - (m_0/B_0\tau)$
J = number of species present
K_1 = a constant in Eq. 20
$k_{nuc}^{ii}, k_{nuc}^{iii}, k_{nuc}^{iv}, k_{nuc}^{v}$ = rate constants for nucleation, $kg^{-1}\ s^{-1}$
k = a stream number
k = iteration number
k_a = area shape factor
k_{break} = rate constant for breakage, $m^{-3}\ s^{-1}$
k_c = mass-transfer coefficient, ms^{-1}

k_{grow} = rate constant for growth, ms^{-1}
k_V = volume shape factor
K = number of streams
l = particle size, m
l_0 = cut size for classification, m
m = mass of crystal, kg
m_0 = zeroth moment
m_3 = third moment
M_c = mass of crystal precipitated, kg
M_{c_calc} = predicted mass of crystal precipitated, kg
M_{cmax} = maximum mass of solute available, kg
M_R = relative molar mass
M_T = suspension density, kg m^{-3}
$n(l)$ = number density, m^{-4}
n_{eq} = number of size classes
$\dot{n}_{LT}$ = total molar flow of liquid, mol s^{-1}
$\dot{n}_{ST}$ = total molar flow of solid, mol s^{-1}
$\dot{n}_T$ = total molar flow, mol s^{-1}
$\dot{n}_j$ = molar flow of species j, mol s^{-1}
Ne = power number (also known as Newton number)
N_i = number of particles per unit volume in size class i, m^{-3}
N_{imp} = impeller frequency, s^{-1}
P = pressure, Pa
q = heat flow, W
q = parameter determining the fineness of the discretization
Q = flow rate of feed slurry to the hydrocyclone (Eq. 19), $m^3\ h^{-1}$
Q = volumetric flow rate (L min^{-1} in Eq. 20), $m^3\ s^{-1}$
$r[n(\cdot), l, \mathbf{s}]$ = density functional describing rate of destruction of particles, $m^{-4}\ s^{-1}$
r = discretization ratio, Eq. 40
r_3 = rate of destruction of third moment, s^{-1}
R_i = rate of destruction of particles in interval i; the discrete equivalent of $r[n(\cdot), l, \mathbf{s}]$
Re = Reynolds number
S = supersaturation ratio
Sc = Schmidt number
Sh = Sherwood number
$S(l, \mathbf{s})$ = selection rate constant for breakage, s^{-1}
t = time (s) and time dependency for breakage frequency
T = temperature, K
u_{mc} = transform of M_c in Eq. 78
V = tank volume, m^3
V = volumetric percentage of solids in the feed to a hydrocyclone, Eq. 19
V_m = molar volume of the aqueous phase from calculated from supersaturation, m^3
w = mass fraction of solute
x = mol fraction
x = particle size, m
$y(\mathbf{l}, \mathbf{s})$ = selection function or grade efficiency for classification

Vectors

$\mathbf{A}$ = a vector of coefficients, Eq. 57
$\mathbf{B}$ = a matrix of coefficients, Eq. 57
$\mathbf{C}$ = a matrix of coefficients, Eq. 57
$\mathbf{E}$ = a tridiagonal matrix, Eq. 58
$\mathbf{F}$ = an upper right triangular matrix, Eq. 58
$\dot{X}\boldsymbol{\xi}$ = vector of reaction rates, mol $m^{-3}\ s^{-1}$
$\mathbf{l}$ = list of particle sizes, Eq. 37
$\mathbf{N}$ = a list of particle numbers Eq. 38
$\boldsymbol{\nu}$ = matrix of stoichiometric coefficients
$\dot{\mathbf{n}}_L = (\dot{n}_{L_1}, \dot{n}_{L_2}, \ldots, \dot{n}_{L_J})$ = species molar flow in the liquid, mol s^{-1}
$\dot{\mathbf{n}}_S = (\dot{n}_{S_1}, \dot{n}_{S_2}, \ldots, \dot{n}_{S_J})$ = species molar flow in the solid, mol s^{-1}
$\dot{\mathbf{n}}_V = (\dot{n}_{V_1}, \dot{n}_{V_2}, \ldots, \dot{n}_{V_J})$ = species molar flow in the vapor, mol s^{-1}
$\mathbf{r}$ = location in physical space for breakage frequency
$\mathbf{s}$ = a vector of conditions describing the solution, such as supersaturation, temperature, etc.
$\mathbf{x}$ = vector of mol fractions

Greek letters

β_0 = size-independent portion of aggregation rate constant, $m^3\ s^{-1}$
β = aggregation rate constant, $m^3\ s^{-1}$
δ = Dirac delta distribution
δ = diffusion layer thickness, m
Δ_p = defined in Eq. 51
Δ = error in Eq. 36
ε = specific power input, W kg^{-1}
Φ_w = weight percent solids in the feed slurry to a hydrocyclone, Eq. 20
λ = particle size, m
λ_{nuc} = rate constant for secondary nucleation, $m^3\ kg^{-1}$
ν_L = kinematic viscosity of the liquid, $m^3\ s^{-1}$
ρ_S = solids density, kg m^{-3}
ρ_m = molar density of particles, mol m^{-3}
ρ_L = liquid density, kg m^{-3}
ρ = density, kg m^{-3}

Subscripts and superscripts

agg = aggregation
break = breakage
grow = growth
I = exponent for concentration or supersaturation in nucleation and growth rate equations
i = size interval number
in = inlet streams
J = exponent for suspension density in nucleation and growth rate equations
k = stream number
L = liquid
m = exponent in volume-dependent breakage rate equation
ngd = nucleation, growth, and dissolution
nuc = nucleation
out = outlet streams
S = solid
T = total
V = vapor
vap = vapor

Literature Cited

1. Hulbert HM, Katz S. Some problems in particle technology: A statistical mechanical formulation. *Chem Eng Sci.* 1964;19:555.
2. Randolph AD, Larson MA. Transient and steady state size distributions in continuous mixed suspension crystallizers. *AIChE J.* 1962;8:639-645.
3. Randolph AD, Larson MA. A population balance for countable entities. *Can J Chem Eng.* 1964;42:280-281.
4. Randolph A, Larson M. In: Mullin JW, ed. *Theory of Particulate Processes: Analysis and Techniques of Continuous Crystallization*. London, UK: Academic Press; 1993.
5. Ramkrishna D. The status of population balances. *Rev Chem Eng.* 1985;3:49-95.
6. Ramkrishna D. *Population Balances. Theory and Applications to Particulate Systems in Engineering*. San Diego, CA: Academic Press; 2000.
7. Hounslow MJ, Wynn E. Short-cut models for particulate processes. *Comput Chem Eng.* 1993;17:505-516.
8. *Stream Analyzer V1.2*. Morris Plains, NJ: OLI Systems Inc.; 2003.
9. *Aspen Plus*. Cambridge, MA: Aspen Technology Inc.; 2002.
10. Hounslow MJ, Mumtaz HS, Collier AP, Bramley AS. A micro-mechanical model for the rate of aggregation during precipitation from solution. *Chem Eng Sci.* 2001;56:2543-2552.
11. Bermingham SK, Kramer HJM, van Rosmalen GM. Towards on-scale crystalliser design using compartmental models. *Comput Chem Eng.* 1998;22:S355.

12. Volmer M, Weber A. Keimbildung in übersättigten Gebilden. *Z Phys Chem* (*Leipzig*). 1926;119:277.
13. Turnball D, Fisher JC. Rate of nucleation in condensed system. *J Chem Phys.* 1965;17:71.
14. Miers HA, Isaac F. The refractive indices of crystallising solutions, with special reference to the passage from the metastable to the labile condition. *J Chem Soc Lond.* 1906;89:413.
15. Garside J. The concept of effectiveness factors in crystal growth. *Chem Eng Sci.* 1971;26:1425-1431.
16. Sohnel O, Garside J. *Precipitation: Basic Principles and Industrial Application*. Oxford, UK: Butterworth–Heinemann; 1992.
17. Puel F, Fevotte G, Klein JP. Simulation and analysis of industrial crystallisation processes through multidimensional population balance equations. Part 1: A resolution algorithm based on the method of classes. *Chem Eng Sci.* 2003;58:3715.
18. Garside J. Industrial crystallisation from solution. *Chem Eng Sci.* 1985;26:1425-1431.
19. Gahn C, Mersmann A. Brittle fracture in crystallization processes. Part A. Attrition and abrasion of brittle solids. *Chem Eng Sci.* 1999;54: 1273-1282.
20. Bermingham S, Verheijen P, Kramer H. Optimal design of solution crystallization processes with rigorous models. *Trans IChemE.* 2003; 81:893-903.
21. Eek RA, Dijkstra SJ, van Rosmalen GM. Dynamic modeling of suspension crystallizers using experimental data. *AIChE J.* 1995;41: 571.
22. O Meadhra R, Kramer HJM, van Rosmalen GM. A model for secondary nucleation in a suspension crystallizer. *AIChE J.* 1996;42:973.
23. Ottens EPK, Janse AH, de Jong EJ. Secondary nucleation in a stirred vessel cooling crystalliser. *J Crystal Growth.* 1972;13/14:500.
24. McCabe WL. Crystal growth in aqueous solutions. *Ind Eng Chem.* 1929;21:30.
25. Giulietti M, Seckler MM, Derenzo S, Ré MI, Cekinski E. Industrial crystallization and precipitation from solutions: State of the technique. *Braz J Chem Eng.* 2001;18:423-440.
26. Mullin JW. *Crystallization*. Oxford, UK: Butterworth–Heinemann; 1997.
27. Branson SH. Factors in the design of continuous crystallisers. *Br Chem Eng.* 1960;5:838.
28. Canning TF, Randolph AD. Some aspects of crystallization theory: Systems that violate McCabe's Delta L law. *AIChE J.* 1967;13:5.
29. Abegg CF, Stevens JD, Larson MA. Crystallization size distribution in continuous crystallizers when growth rate is size dependent. *AIChE J.* 1968;14:118.
30. White ET, Wright PG. Magnitude of size dispersion effects in crystallization. *Chem Eng Prog Symp Ser.* 1971;67:81.
31. Larson MA, White ET, Ramarayanan KA, Berglund KA. Proc of 75th Annual Meeting of AIChE, Los Angeles, CA; 1982.
32. Human HJ, van Enekevork WJP, Bennema P. *Industrial Crystallisation 81*. Amsterdam: North-Holland; 1982.
33. Smoluchowski MV. Mathematical theory of kinetics of the coagulation of colloidal solutions. *Z Phys Chem.* 1917;92:129.
34. Sastry KVS. Similarity size distribution of agglomerates during their growth by coalescence in granulation or green pelletization. *Int J Miner Process.* 1975;2:187.
35. Bramley A, Hounslow M. Aggregation during precipitation from solution: A method for extracting rates from experimental data. *J Colloid Interface Sci.* 1996;183:155.
36. Prasher CL. *Crushing and Grinding Process Handbook*. New York, NY: Wiley; 1987.
37. Nicmanis M, Hounslow M. Finite-element methods for steady-state population balance equations. *AIChE J.* 1998;44:2258-2272.
38. Hounslow M, Pearson J, Instone T. Tracer studies of high-shear granulation: II. Population balance modeling. *AIChE J.* 2001;47:1984-1999.
39. Attarakih MM, Bart HJ, Faqir NM. Optimal moving and fixed grids for the solution of discretized population balances in batch and continuous systems: Droplet breakage. *Chem Eng Sci.* 2003;58:1251-1269.
40. Plitt LR, Kawatra SK. Estimating the cut (d50) size of classifiers without product particle-size measurement. *Int J Miner Process.* 1976; 5:364-378.
41. Wills BA. *Mineral Processing Technology*. Oxford, UK: Butterworth–Heinemann; 1997.
42. Lynch AJ, Rao TC. Modelling and scale-up of hydrocyclone classifiers. Proc of 11th Mineral Processing Congress, Cagliari, Italy; 1975.
43. Kramer HJM, Bermingham SK, van Rosmalen GM. Design of industrial crystallisers for a given product quality. *J Cryst Growth.* 1999; 198/199:729-737.
44. Jager J. *Control of Industrial Crystallisers; the Physical Aspects.* PhD Thesis. Delft, The Netherlands: Delft University of Technology; 1990.
45. Kumar S, Ramkrishna D. On the solution of population balance equations by discretization—III: Nucleation, growth and aggregation of particles. *Chem Eng Sci.* 1997;52:4659-4679.
46. Kiparissides CA, Alexopoulos AH. Solution of PBEs for prediction of PSD in particulate systems: Effect of combined nucleation, growth and aggregation. Industrial Processes of Particle Formation. Proc of AIChE 2002 Annual Meeting, Indianapolis, IN, Nov. 3–8; 2002.
47. Hounslow MJ, Ryall RL, Marshall VR. A discretized population balance for nucleation, growth, and aggregation. *AIChE J.* 1988;34: 1821.
48. Litster J, Smit D, Hounslow M. Adjustable discretized population balance for growth and aggregation. *AIChE J.* 1995;41:591-603.
49. Wynn EJW. Improved accuracy and convergence of discretized population balance of Lister et al. *AIChE J.* 1996;42:2084-2086.
50. Hounslow MJ. A discretized population balance for continuous systems in a steady state. *AIChE J.* 1990;36:106-116.

Manuscript received Nov. 5, 2004, and revision received Feb. 21, 2005.